Available online at www.sciencedirect.com
SCIENCE DIRECT®
Geomorphology 74 (2006) 152–163
GEOMORPHOLOGY
www.elsevier.com/locate/geomorph

Surficial patterns of debris flow deposition on alluvial fans in Death Valley, CA using airborne laser swath mapping data

Dennis M. Staley [a,b,*], Thad A. Wasklewicz [a], Jacek S. Blaszczynski [c]

[a] Department of Earth Sciences–Geography, University of Memphis, Memphis, TN 38152, USA
[b] USDA Forest Service, Renewable Resources, Golden, CO 80401, USA
[c] USDI Bureau of Land Management, National Science and Technology Center, Denver, CO 80225, USA

Received 28 April 2005; received in revised form 15 July 2005; accepted 15 July 2005
Available online 10 October 2005

Abstract

Debris flows are a common event in mountainous environments. They often possess the greatest potential for destruction of property and loss of lives in these regions. Delimiting the spatial extent of potential damage from debris flows relies on detailed studies of the location of depositional zones. Current research indicates debris flow fans have two distinct depositional zones. However, the two zones were derived from studies containing detailed analyses of only a few fans. High resolution airborne laser swath mapping (ALSM) data is used to calculate profile curvature and surface gradient on 19 debris flow fans on the eastern side of Death Valley. The relationship between these parameters is assessed to 1) identify if debris flow fans are accurately represented by two depositional zones, and 2) to assess how these terrain parameters relate to one another at the individual fan scale. The results show at least three zones of deposition exist within the sampled fans. These zones do not hold consistent when individual fan morphometry is analyzed in conjunction with localized fan surface gradients. Fans with consistently shallower gradients exhibit numerous depositional zones with more subtle changes in profile curvature. Steeper gradient fans exhibit significantly fewer zones with more pronounced local changes in profile curvature. The surface complexity of debris flow fans is evident from these analyses and must be accounted for in any type of hazard studies related to these features.

Keywords: Debris flow; Alluvial fan; Death Valley; ALSM; LiDAR; Morphometry

1. Introduction

The importance of debris flows in alluvial fan development has been recognized since the 1920s (Blackwelder, 1928). Recently, debris flows and society have become more intertwined as urban sprawl and a desire of individuals to move to cooler, secluded locations with a view has brought more people into areas prone to debris flow events. Debris flows and floods are two of the most destructive phenomena tied to human development on alluvial fans (Larsen et al., 2001). One of the important factors in understanding the potential hazards associated with active debris flow processes on fans and equally important in regards to fan evolution is determining the spatial patterns of debris flow deposition. The spatial variability of debris flows have been examined by two basic approaches: field-based methods (Okuda and Suwa, 1981; Suwa and Okuda, 1983; Whipple and Dunne, 1992), and physical and mathematical modeling (Lancaster et al., 2003; Major and Iverson, 1999). However, these techniques do not

* Corresponding author. Department of Earth Sciences–Geography, University of Memphis, Memphis, TN 38152, USA. Tel.: +1 303 783 4781; fax: +1 303 275 5075.
E-mail address: dstaley@memphis.edu (D.M. Staley).

0169-555X/$ - see front matter © 2005 Elsevier B.V. All rights reserved.
doi:10.1016/j.geomorph.2005.07.014

adequately assess the spatial variability of debris flow processes and associated hazards on fan surfaces beyond a localized scale (Costa, 1984). Instead, the spatial patterns of debris flow processes can be assessed using measurements of fine-scale surface morphometry.

Surficial features (e.g., levees, lobes, debris dams, and channels) identified on many fans result from variations in debris flow processes. Several researchers have identified two distinct zones of deposition on debris flow fans (Suwa and Okuda, 1983; Whipple and Dunne, 1992). An upper fan depositional zone exhibits rough topographic features that result from clast-supported flows that deposit near the fan apex (Suwa and Okuda, 1983). Distal fan locations display smoother surface topography generated by finer matrix-supported deposits that thin as they flow over longer distances (Suwa and Okuda, 1983). These zones reflect intricate relationships between debris flow processes (rheology, sediment concentration) and form (channel dimensions, local gradient).

Two varying approaches have been employed in the assessment of process–form relationships in debris flow fans. Okuda and Suwa (1981) and Suwa and Okuda (1983) examined runout distances as they related to debris flow velocities along the length of the fan. These authors identified variations in surface relief through time and how these topographic changes influenced the loci of deposition in subsequent events. Whipple and Dunne (1992) studied debris flow sediment concentrations as they relate to channel processes and rheological characteristics. While these studies provide a framework for the analysis of spatial distribution of debris flow deposition, they have been conducted using a limited number of sampling locations within individual fans and, therefore, do not assess variations between fans. The availability of airborne laser swath mapping data (ALSM) allows for high-resolution modeling of fan topography. Morphometric parameters of gradient and profile curvature are derived from these data. Here we utilize fine-scale morphometric measurements to map debris flow deposition and determine if the two zones of deposition are consistent between multiple alluvial fans in Death Valley, California, USA. We postulate that the current assertion of two depositional zones is an oversimplification of the complex, nonlinear processes acting upon these surfaces.

2. Study area

This research focuses on debris flow fans in the eastern central portion of Death Valley National Park, California, USA. The central portion of Death Valley is an extensional basin bounded by the Black Mountains to the east and the Panamint Range to the west. Fans on the eastern edge of the valley at this location are Holocene in age. At a coarse spatial scale, debris flow fans in the study area represent a continuum between steep, topographically complex surfaces exhibiting a high degree of "swollenness" of deposits and lower gradient surfaces with lesser topographic complexity with "flatter" deposits. While the mean values of gradient and curvature may reflect broad-scale trends of the fan surface and formative processes, these global values fail to identify fine-scale variability of process and form within each fan (Table 1). At this scale, field observations and map interpretation indicate the fans are comprised of lobate deposits of varying thickness and length occurring at various intervals along the distance of the fans. The morphometry of these deposits and the downfan distance also varies between the fans in the study area.

As this study analyzes the potential linkage between fan form and debris flow process, care must be taken to reduce the influence of other processes on curvature values. A careful visual analysis of each debris flow fan was employed to eliminate sections of fans from the analysis set if the curvature values were influenced by tectonic processes, vegetation growth, or anthropogenic influences. For example, DF08 shows evidence of the surface expression of a north–south trending fault (Fig. 1A). Curvature values immediately upslope of the fault scarp are highly convex (positive curvature), while

Table 1
Mean fan and basin morphometry parameters

Fan name	Fan area (km^2)	Mean fan gradient (°)	Mean fan profile curvature	Basin area (km^2)
DF01	0.193	9.715	0.048	1.008
DF02	0.028	16.242	0.118	0.204
DF03	0.684	5.859	0.059	5.730
DF04	0.012	15.534	0.307	<0.080
DF05	0.015	14.457	0.284	0.083
DF06	0.058	12.759	0.163	0.304
DF07	0.188	7.247	0.059	0.677
DF08	0.015	19.030	0.261	0.086
DF09	0.021	23.628	0.263	0.128
DF10	0.011	19.009	0.381	0.108
DF11	0.022	12.614	0.292	0.200
DF12	0.065	8.593	0.091	0.960
DF13	0.033	11.606	0.111	0.290
DF14	0.010	15.884	0.299	0.084
DF15	0.011	11.695	0.264	0.149
DF16	0.012	14.153	0.286	0.082
DF17	0.061	8.617	0.104	0.460
DF18	0.072	13.152	0.121	0.487
DF19	0.034	10.414	0.140	0.338

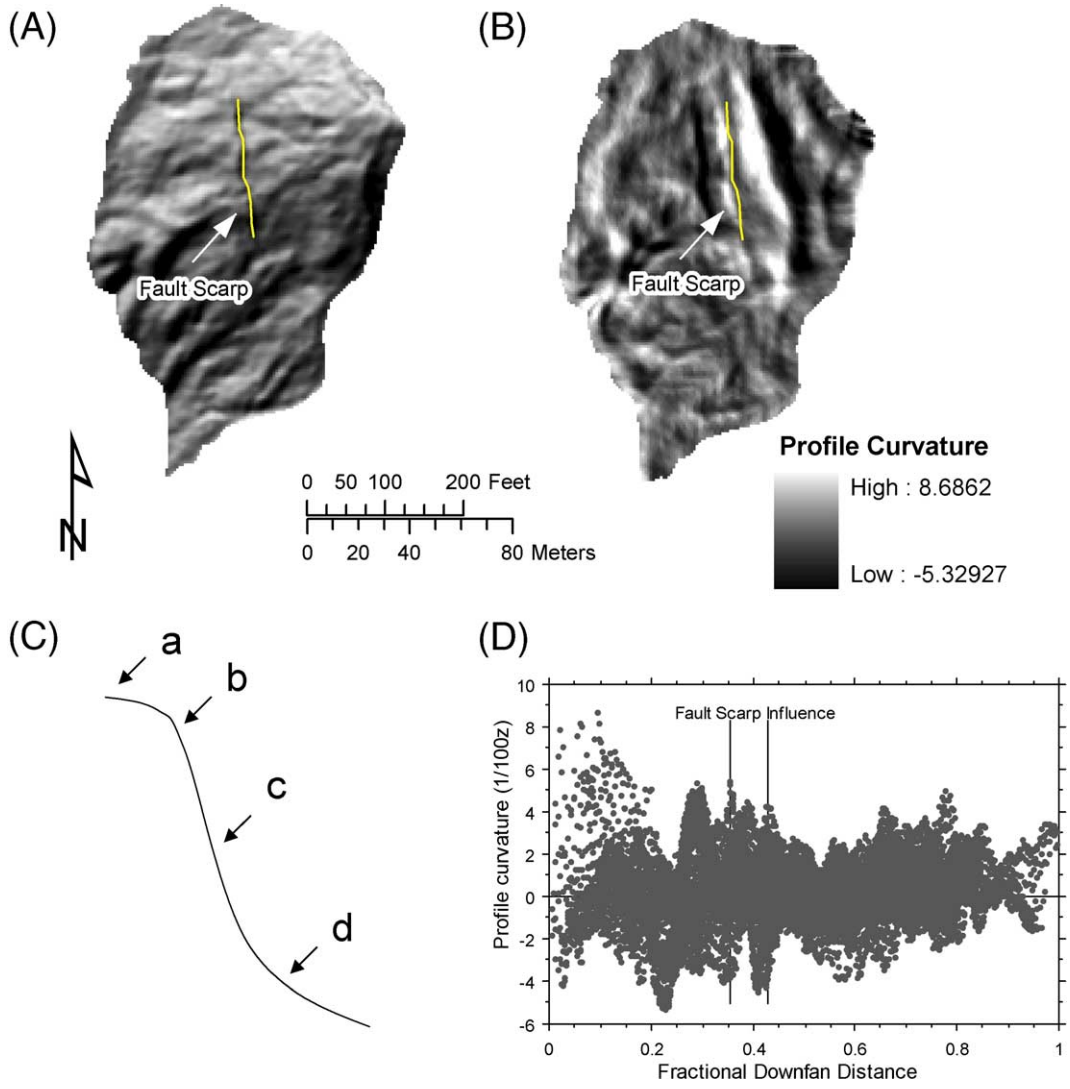

Fig. 1. Fault scarp influence on profile curvature. (A) Shaded relief map where contours represent fractional downfan distances; (B) profile curvature map where dark tones indicate negative curvature, light tones indicate positive curvature; (C) graphic representation of fault scarp where point A represents a slightly convex surface, point B represents a highly convex surface, point C represents a rectilinear surface and point D represents a basal concavity; (D) a scattergram plotting profile curvature against fractional downfan distance; fault scarp influence on relationship is identified.

curvature values immediately downslope of the fault scarp are highly concave (negative curvature) (Fig. 1B). These values are consistent with curvatures that one would expect to find along a scarp (Fig. 1C); upper slopes near-rectilinear (a), a sharp increase in gradient (strong convexity) at the head of the scarp (b), a near-rectilinear scarp face (c), and a sharp decrease in slope (strong concavity) at the foot of the scarp (d). These large curvature values (both positive and negative) are reflected in a scattergram plotting profile curvature against fractional downfan distance (Fig. 1D). Curvature values displayed in this fashion may "peak" at fault scarps. The potential exists for processes other than those associated with debris flows to produce distinct peaks of curvature values. However, careful visual analysis has revealed that these processes are readily identifiable from combined analysis of shaded relief and curvature maps. Therefore, individual sections of fans where form has been influenced by other processes are excluded from this type of analysis.

In all, 19 fans were selected for inclusion in this analysis as they exhibited minimal surficial expression of tectonic processes, anthropogenic influences, or vegetation growth (Fig. 2). The four fans consistently

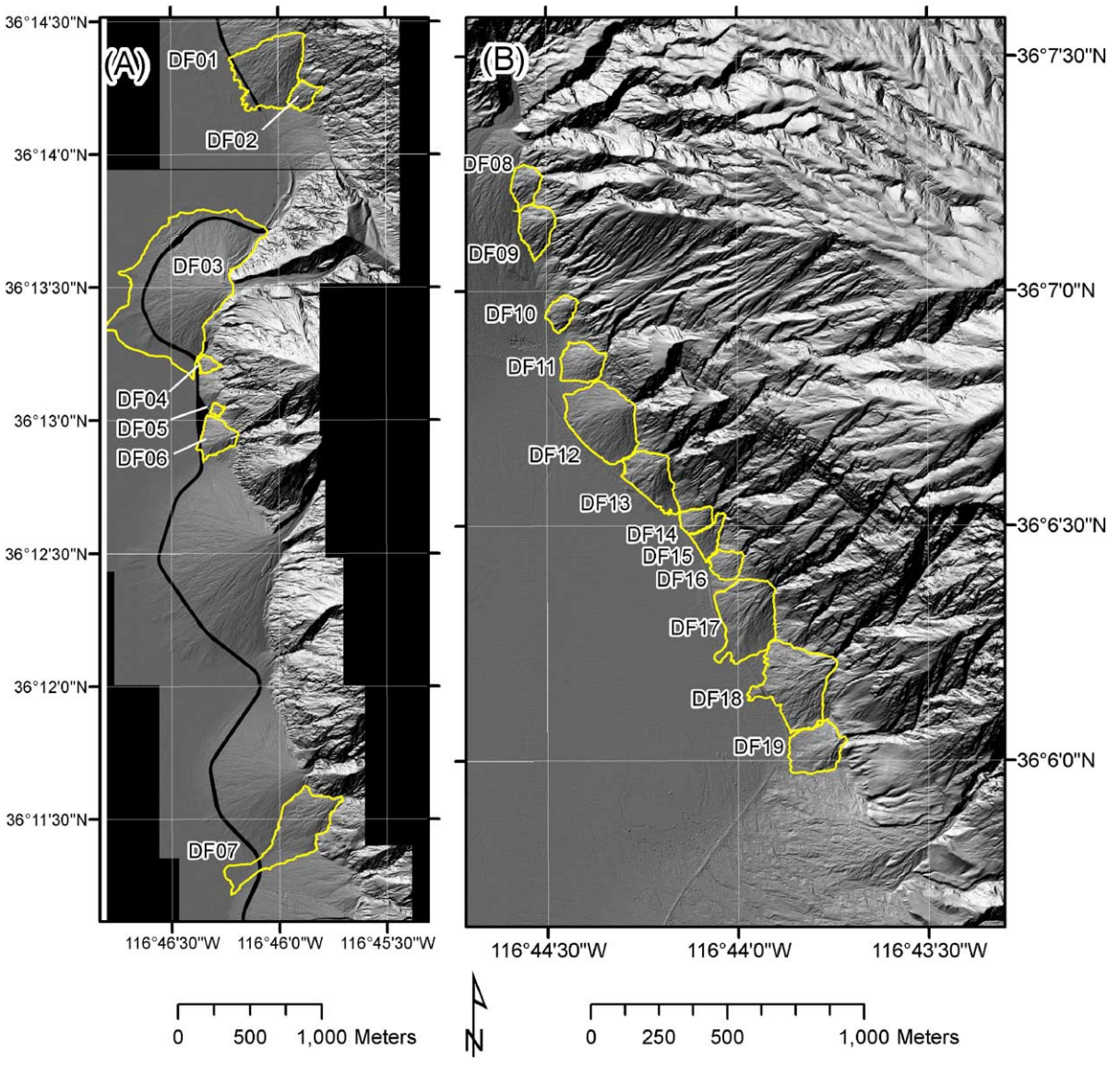

Fig. 2. Nineteen debris flow fans on the eastern side of Death Valley, California, USA. Fans selected for detailed analysis include DF09, DF12, DF14 and DF19.

discussed in this article (DF09, DF12, DF14, DF19) are considered representative of all fans included in the analysis.

3. Methods

3.1. Data collection

All ALSM data used for this project were generated by the NSF-supported National Center for Airborne Laser Mapping (NCALM) contained within the University of Florida's Department of Civil and Coastal Engineering. Data were gathered over a 3-d period: 29 May, 30 May, and 2 June 2003. The mountainous topography dictated the flight altitude, which ranged between 300 and 1100 m above ground level. Data acquisition used the following parameters: a scan angle of 20° (1/2 FOV); a scan frequency of 28 Hz, and a pulse rate of 33,333 Hz. Post-processing of all ALSM data was conducted at NCALM. Data were received as ASCII files that contain *X*, *Y*, and *Z* triplets processed from laser shots. Laser shots were obtained by using a kriging algorithm on separate flight strips that overlapped at greater than 30%. Grid nodes were combined with a weighted scheme based on strip geometry to produce a best estimate of elevation on a 1-m

grid. All analyses were conducted from 1-m raster grids generated directly from 1-m grid nodes. The 1-m raster grids were imported into ArcInfo Workstation for calculation of morphometric parameters and spatial analysis.

3.2. Morphometry

The morphometric parameters of surface gradient and profile. Morphometric parameter values were calculated using a modified version of the slopeshapes.aml algorithm developed by Blaszczynski (1997). This method generalizes the slope to calculate curvature at user-defined length scales. Generalization of data is obtained by applying the FOCALMEAN function to the original DEM and by increasing the radius of the circle at regular intervals. All calculations were performed in ArcInfo GRID. In order to minimize the edge effects associated with morphometric parameter derivation, parameters were derived for the entire ALSM data area and subsequently clipped to the individual fan surface.

Gradient is the first derivative of elevation and is defined as the change in elevation over a specified distance (represented by degrees). In order to assess the influence of gradient on curvature values, the length-scale at which gradient is calculated must be significantly greater than that used to calculate profile curvature. Gradient was calculated at an 11-m length scale. The 11-m length scale was selected as it was greater than the length scale of the debris flow lobes and levees. Therefore, broad surface trends were still evident, yet finer scale features were generalized. Gradient is important in the processes associated with debris flow events, as it is inversely related to the shear strength of the flow and positively correlated with the shear stresses associated with the flow (Costa, 1984; Parsons et al., 2001). Snouts with greater shear strengths are able to maintain debris dams at higher gradients than those with lower shear strengths (Costa, 1984; Parsons et al., 2001).

Profile curvature was calculated at a 5-m length scale following a slope generalization algorithm modified from Blaszczynski (1997). Notably, the magnitude and sign of the value reflect the shape of the surface. Positive curvature values reflect upwardly convex surfaces, while negative curvature values reflect upwardly concave surfaces (Blaszczynski, 1997). Fig. 3 illustrates the concept of profile curvature along transect ABC. Curvature values increase until point a_1, decrease from a_1 to b_1, and increase again (but remain negative) throughout the remainder of the surface. Debris flow deposits are characterized by a main body that can be slightly convex, slightly concave, or rectilinear and by snout-like (lobate) forms comprised of interlocking, coarse grains (Costa, 1984; Parsons et al., 2001; Suwa and Okuda, 1983). In profile, these snouts tend to have an upper convexity, a lower near-rectilinear face, and a lower concavity. The shape of these snouts [i.e., "swollenness" after Okuda and Suwa (1981) and Suwa and Okuda (1983)] is a product of the shear strength associated with the frictional locking grains at the snout front (Parsons et al., 2001). Snouts with high internal shear strength will act as a debris dam. Behind the debris dam, the fluid pressure of the flow will increase until the dam is overtopped, moved further downslope, or the flow is stopped behind the dam if the shear strength of the snout is greater than the maximum shear stresses associated with the debris flow (Costa, 1984; Parsons et al., 2001). Profile curvature reflects the relationship between these shear stresses and shear strengths. As fluid pressure and shear stress build be-

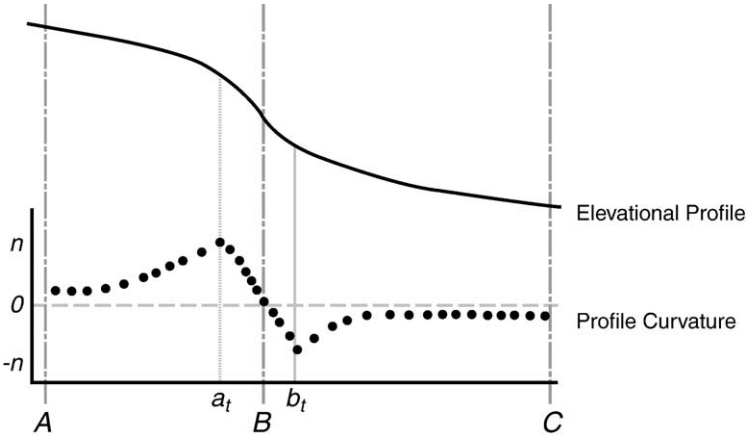

Fig. 3. Relationship between profile curvature and the elevational profile of an idealized surface.

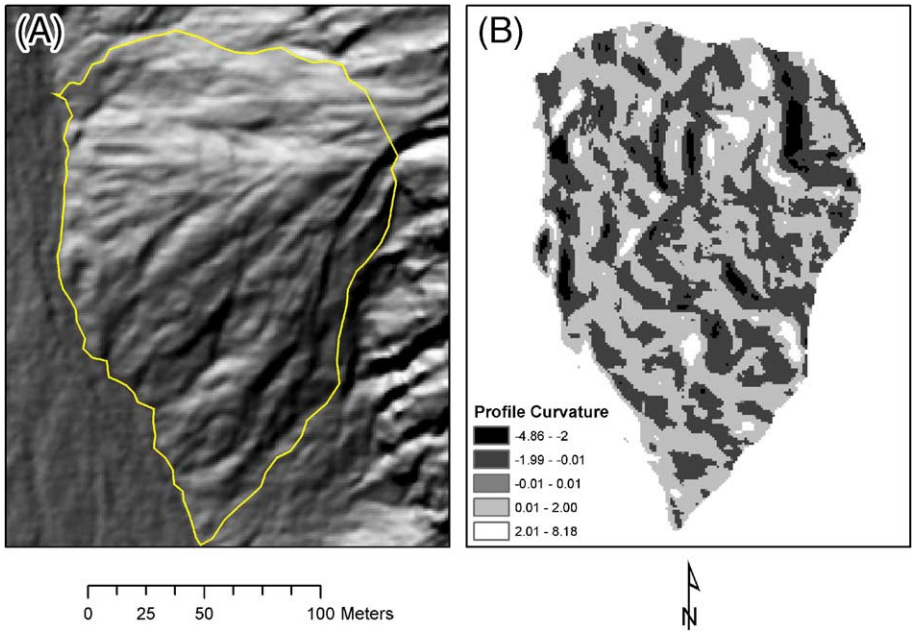

Fig. 4. DF09: (A) Shaded relief map; (B) profile curvature map.

hind debris dams, the dams grow in size. The greater the internal shear strength of the snout and the higher the fluid pressure and shear stress of the flow, the more pronounced the thickness (Costa, 1984). The thickness or swollenness will be reflected in a greater dispersion of the profile curvature values associated with the snout. These snouts with a "swollen" or "thick" appearance exhibit greater curvature values (e.g., greater rates of change of slope) than the runout areas and the main body of the debris flow. Magnitude of the curvature values would be expected to be greater on the convex upper snout than the concave lower snout, as the rate of change of slope is minimized at the base of the snout because of the gradient of the fan surface. Fig. 4 illustrates the profile curvature of DF09.

Table 2
Fractionated downfan distance zones

Zone	Fractionated distance ranges	Zone	Fractionated distance ranges
5	$0.00 < df \leq 0.05$	55	$0.50 < df \leq 0.55$
10	$0.05 < df \leq 0.10$	60	$0.55 < df \leq 0.60$
15	$0.10 < df \leq 0.15$	65	$0.60 < df \leq 0.65$
20	$0.15 < df \leq 0.20$	70	$0.65 < df \leq 0.70$
25	$0.20 < df \leq 0.25$	75	$0.70 < df \leq 0.75$
30	$0.25 < df \leq 0.30$	80	$0.75 < df \leq 0.80$
35	$0.30 < df \leq 0.35$	85	$0.80 < df \leq 0.85$
40	$0.35 < df \leq 0.40$	90	$0.85 < df \leq 0.90$
45	$0.40 < df \leq 0.45$	95	$0.90 < df \leq 0.95$
50	$0.45 < df \leq 0.50$	100	$0.95 < df \leq 1.00$

Fractional downfan distances (D_f) were calculated to assist in the analysis of the spatial location and patterns of profile curvature values. The fractional downfan distance was calculated for each cell based upon planimetric (horizontal) distance from the fan apex, and is represented by the equation:

$$D_f = D_a / D_{max} \quad (1)$$

where D_f represents the fractional downfan distance, D_a represents the planimetric distance to from the cell to the apex, and D_{max} represents the maximum planimetric distance to apex within the entire fan surface. Values range from 0 to 1, with the apex representing $D_f=0$, and the farthest grid cell within the fan representing $D_f=1$. For analyses requiring discrete data, the fractional distance values were divided into 5% zones (Table 2).

3.3. Analysis

Morphometric parameters derived from 1-m ALSM data were analyzed at fine and coarse scales. Fine-scale analyses of morphometric variability within each fan are intended to elucidate differences in debris flow processes between each fan. Coarse-scale analyses including all fans are intended to identify general trends in debris flow processes and morphometry within the study area. These findings are compared to the results obtained by Suwa and Okuda (1983) and Whipple and Dunne (1992).

Scattergrams were utilized as a means of visualizing the relationships between i) curvature and fractional downfan distance and ii) curvature and gradient. The relationship between profile curvature and gradient was analyzed to determine if the slope of the surface could exert some control over the spatial distribution of debris flow process. Plotting profile curvature against regional gradient would allow for the visualization of thresholds between these two parameters. The relationships between fractional downfan distance, profile curvature, and gradient were analyzed to determine if the spatial patterns of these parameters were similar within and between fans. Plotting profile curvature against the fractional downfan distance permits identification of areas of rapidly changing curvature, such as those associated with the snouts of debris flow lobes.

The relationship between downfan distance (in 5% zones), mean zone gradient, and the within-zone standard deviation of profile curvature are visualized using box plots. These plots aid in the interpretation of broad scale trends of surface gradient and ranges of profile curvature. Correlation analysis between mean gradient and the standard deviation of profile curvature for each zone is intended to elucidate zones of deposition that exhibit similar process-form relations. Mean zone curvature is intended to represent the overall trend of the fan gradient within each zone. The standard deviation of curvature is intended to represent the overall "swollenness" of deposits within the fan zone. Zones with a high standard deviation exhibit a higher degree of topographic complexity than those with lower standard deviations. This analysis is intended to assess how many depositional zones are evident at a broad scale when data from all 19 fans are combined.

4. Results

The results of this analysis are divided into three categories. At the individual fan scale, the relationships between gradient and profile curvature and the relationships between profile curvature and fractional downfan distance are presented. At a coarser spatial scale, results are presented from inclusion of all 19 fans within the study area. This section illustrates the general relationships between the standard deviation of profile curvature, mean gradient, and fractional downfan distance zone.

4.1. Fine scale analysis: gradient vs. profile curvature

When plotted as a scattergram, the relationship between regional gradient and local curvature is quite complex. "Peaks" in the scattergram are interpreted as areas of deposition. Peaks suggest the uppermost portion of a "swollen" deposit similar to those described by Okuda and Suwa (1981) and Suwa and Okuda (1983), while "valleys" represent the basal concavities associated with these deposits. These assumptions have been validated by field observation.

DF09 (Fig. 5A) exhibits at least three peaks: approximately 34°, 25°, and 15°. The scattergram depicting the relationship between profile curvature and gradient for fan DF12 is decidedly different than that of DF09. Apparently, a curvilinear relationship exists between these terrain parameters (Fig. 5B). DF14 exhibits peaks in curvature at gradients >30°, ~22.5°, and a slight peak between 10° and 12.5° (Fig. 5C). DF19 exhibits peaks at ~25° and 7° (Fig. 5D). The large "valley" depicted at ~23° is interpreted as being the highly concave basal sections of the lobes identified at 25°.

4.2. Fine scale analysis: profile curvature and gradient vs. fractional downfan distance

A complex relationship is also evident when the relationship between profile curvature and fractional downfan distance is plotted as a scattergram. These relationships are further elucidated when compared to a scattergram of gradient against downfan distance. DF09 exhibits several peaks of curvature as distance away from the apex increases (Fig. 6A). The highest magnitude of curvature values are found at fractional distances of 0.10–0.20, 0.65–0.80, and 0.95. This corresponds to the spatial location of the aforementioned curvature peaks associated with maximum gradients of approximately 34°, 25°, and 15° (Fig. 6B). DF12 exhibits peaks in curvature values at fractional distances of 0–0.10, 0.25–0.30, 0.80–0.85, and 0.95–1.0 (Fig. 6C). These peaks are located where maximum gradients fall below 25°, 20°, 10°, and 5°, respectively (Fig. 6D). Peaks in curvature on DF14 occur at fractional distances of 0–0.2, with numerous minor peaks throughout the length of the fan (Fig. 6E). The major peak at 0–0.2 occurs where slope values are >25°, while the minor curvature peaks along the remaining length of the fan follow local increases in gradient (Fig. 6F). DF19 exhibits major peaks in curvature at fractional distances of 0.15–0.30 and 0.60–0.70, with minor peaks occurring throughout the length of the fan surface (Fig. 6G). The major peak between distances of 0.15–0.30 corresponds with a local increase in gradient >20° (Fig. 6H). The other large peak at fractional distances of 0.60–0.70 corresponds with maximum curvature values falling

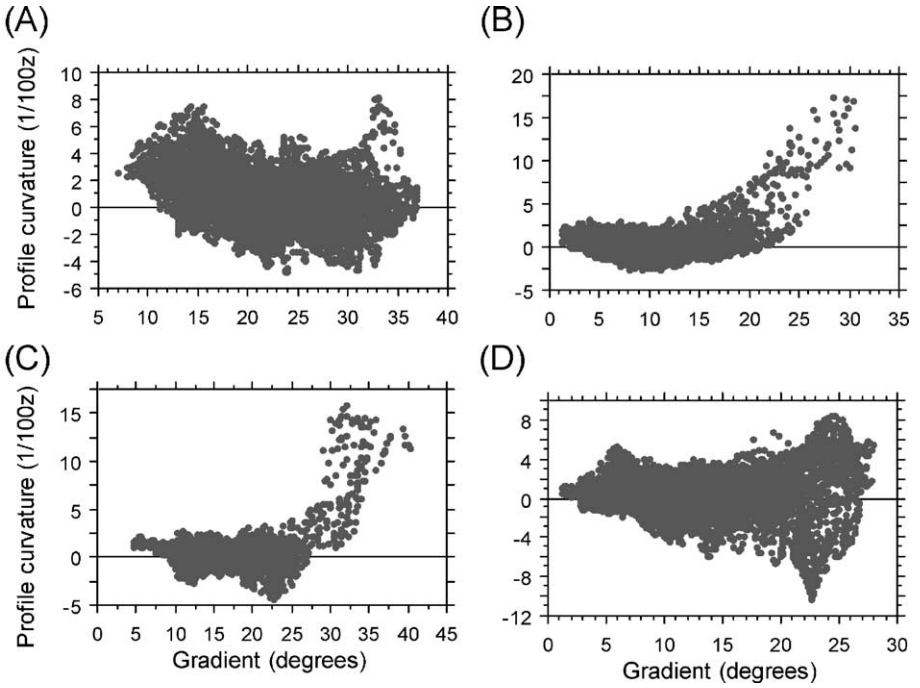

Fig. 5. Scattergrams for gradient and profile curvature: (A) DF09 (n=21,414); (B) DF12 (n=64,668); (C) DF14 (n=10,400); (D) DF19 (n=34,013).

below ~12.5°. The minor peaks throughout the length appear to be related to a gradual decrease in maximum gradient values. These four fans exhibited very little similarity in the downfan location of local increases in profile curvature and surface gradient despite similarities in rock type, tectonic setting, and climate.

4.3. Broad scale analysis: mean gradient and standard deviation of profile curvature by zone

The standard deviation of profile curvature values within each distance zone tends to increase with mean zone gradient (Fig. 7). When represented as a box plot, mean gradient generally decreases with fractional downfan distance zone (Fig. 8A). Sharp decreases in mean gradient are noted in the upper (0.05–0.35) and lower (0.75–1.0) zones. Decreases in mean gradient are much less pronounced in mid sections of the fan surfaces (zone 0.35–0.70).

The standard deviation of profile curvature and fractional downfan distance zone exhibits a more complex relationship (Fig. 8B). Three zones with similar trends are identified. Median values tend to slightly decrease in the downfan direction. The range of standard deviation values is highest at the uppermost portion of the fans (zones 0.05–0.30), decrease in the mid-fan zones (0.40–0.70) and increase again at the distal section of the fans (0.75–1.0). This suggests that at a coarse scale, the 19 debris flow fans are characterized by at least three zones of deposition. At the uppermost section, wide ranges in the standard deviation are indicative of deposits with a range of shear strengths. However, these shear strengths tend to be higher in this section of the fan than in any of the lower sections. Deposits with consistently low ranges of curvature values characterize the mid-fan sections. This correlates with a general runout zone within this section of the fan surfaces, especially on those fans with lower overall gradients. A small peak in the standard deviation of curvature values is identified at the distal section of the fan.

The three zones identified in the analyses of mean gradient and standard deviation of profile curvature are spatially coincident. To test the statistical significance of this relationship, correlation analyses at $\alpha = 0.05$ were utilized (Table 3). No statistically significant correlation was identified for zones 0.05–0.30 or at zone 0.65. Statistically significant correlations were identified for all other zones (0.35–0.60, 0.70–1.0). This suggests that gradient may exert a greater control over the range of profile curvature values at the lower mean gradients associated with the distal sections of the fan surface.

5. Discussion

The current view of debris flow fans having two characteristic depositional zones does not fit the results

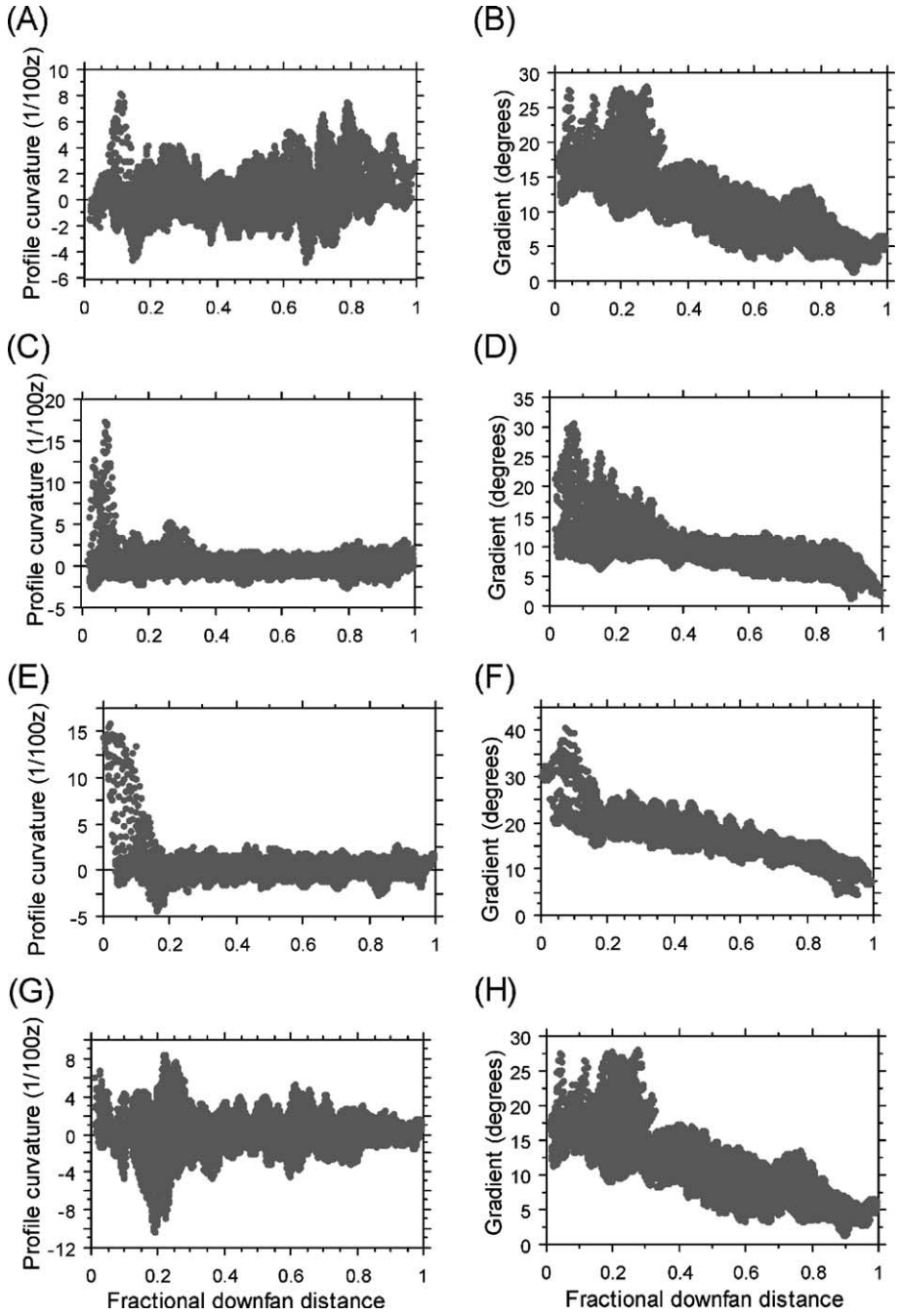

Fig. 6. Scattergrams plotting profile curvature and gradient against fractional downfan distance: (A) DF09, fractional downfan distance vs. profile curvature (n = 21,414); (B) DF09, fractional downfan distance vs. gradient (n = 21,414); (C) DF12, fractional downfan distance vs. profile curvature (n = 64,668); (D) DF12, fractional downfan distance vs. gradient (n = 64,668); (E) DF14, fractional downfan distance vs. profile curvature (n = 10,400); (F) DF14, fractional downfan distance vs. gradient (n = 10,400); (G) DF19, fractional downfan distance vs. profile curvature (n = 34,013); (H) DF19, fractional downfan distance vs. gradient (n = 34,013).

identified in this study. The spatial variability in debris flow deposition along the length of the fan surface is dependent upon the characteristics of the individual fan system. The spatially coincident peaks in gradient and profile curvature reflect thresholds within the relationship between surficial form and depositional processes. The gradient values, at which the curvature values peak, suggest potential depositional threshold values related

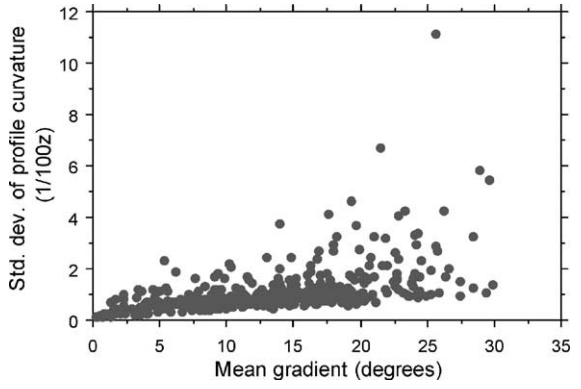

Fig. 7. Standard deviation of curvature increases with mean gradient when calculated for each distance zone ($n=380$).

to the shear strengths and stresses associated with debris flow rheology. As the debris flow surges downfan, debris lobes form along gradients where the shear strength of the surge boundary exceeds the shear strength of the flow (Costa, 1984; Fannin and Rollerson, 1993; Parsons et al., 2001). The locations of the lobes vary between all analyzed fans. Steep fans (e.g., DF09) typically exhibit higher curvature values and a wider variability in curvature than lesser gradient fans (e.g., DF12). Steeper fans also exhibit a fewer number

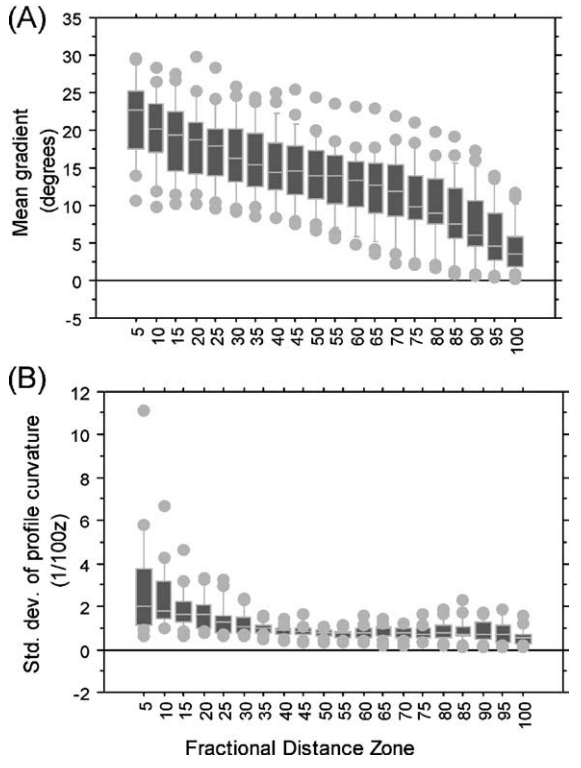

Fig. 8. Data from 19 debris flow fans: (A) Mean gradient by zone and; (B) standard deviation of profile curvature by zone ($n=19$ per zone).

Table 3
Correlations between mean gradient and standard deviation of profile curvature by zone. Bold indicates statistically significant relationship at á=0.05 ($n=19$)

Fractionated distance zone	*R*	*P*-Value
0.05	0.289	0.235
0.10	0.355	0.138
0.15	0.300	0.215
0.20	0.352	0.141
0.25	0.319	0.186
0.30	0.367	0.124
0.35	0.535	**0.017**
0.40	0.462	**0.046**
0.45	0.571	**0.010**
0.50	0.675	**0.001**
0.55	0.683	**0.001**
0.60	0.477	**0.038**
0.65	0.406	0.085
0.70	0.782	<**0.001**
0.75	0.725	**0.000**
0.80	0.613	**0.004**
0.85	0.455	**0.050**
0.90	0.613	**0.004**
0.95	0.661	**0.002**
1.00	0.676	**0.001**

of peaks in curvature values than shallower gradient fans. These peaks in curvature are spatially coincident with the locus of deposition associated with debris flow events.

At a broad scale, the data suggest that there are at least three zones of morphometric differences on the 19 fans included in this study. Gradients tend to be highest at the fan apex and decrease rapidly until a fractional downfan distance of ~0.30. A wide range of curvature values characterizes this zone. On shallow gradient fans, this zone is typified by isolated areas of deposits with high internal shear strengths and, more commonly, of runout zones of events that extended farther downfan. On steeper fans, deposits of high shear strength exhibiting high profile curvature values characterize the high gradient section. Between fractional downfan distances of 0.35 and 0.70, gradients decrease less rapidly than in the proximal segment. In this section, fans exhibit a runout zone punctuated by isolated deposits of lower shear strength. This relationship is much more clearly defined on shallow gradient fans. At the distal section of the fan (0.75–1.0), gradient appears to once again exert significant control on deposit morphometry and process. Gradient decreases rapidly in this section. The range of curvature values in this zone is greater than that of the mid-fan zones for all debris flow fans in the study area.

When the relationship between fan gradient, curvature, and downfan distance are analyzed, a simple

pattern emerges. This pattern suggests that as fan gradient decreases, the number of zones of deposition increases, while the degree of "swollenness" of deposits decreases. This is interpreted as complexity in process-form relations on these 19 fan surfaces. At the temporal scale associated with an individual event, the locus of deposition is controlled by surface gradient and flow rheology. At the temporal scale associated with fan evolution, the overall gradient of the fan surface is controlled by the rheology of the formative events.

The spatial and scalar complexities of the depositional patterns discovered from this study should be considered in hazard management strategies. Distinct areas of debris flow runout and deposition are found in alluvial fans. However, our results also indicate a level of variability within and between fans. Managers should look at fans on a case-by-case basis in the decision making process. The three zones presented here should only be used as a model for guiding management schemes. The long-term inactivity of a surface or the exact location of the three zones can change rapidly. In conjunction with the depositional zones, the coarse-scale fan gradient can be used as a proxy for assessing variability in the model of three depositional zones. The variation through space and time is also linked to factors in the drainage basin as well as the rheologic conditions of the flow. Sediment and water transfer parameters tied to the drainage characteristics vary from flow to flow and likely lead to differences in runout and depositional characteristics and extent. These specific process-oriented data must be also connected to the general zones of debris flow deposition.

6. Conclusions

High resolution ALSM data allowed the calculation of terrain parameters on 19 debris flow fans in Death Valley National Park at an unprecedented spatial scale. At a broad scale, at least three zones of similar depositional processes were identified from morphometric properties. High curvature values suggest high internal shear strength deposits associated with flows that halt at high gradients typical of proximal locations on the fan surface. Mid-fan sections are typified by low curvature values with small standard deviations indicative of runout zones. Low curvature values with a higher standard deviation than the mid-fan section suggest low internal shear strength deposits associated with flows halting at lower gradients. This is characteristic of the distal portion of the fan. These general results are similar to those reported by Suwa and Okuda (1983) and Whipple and Dunne (1992).

However, these findings are not applicable at the scale of individual fan surfaces. The location and number of depositional zones are not consistent within the individual fans. Steeper gradient fans tend to have fewer, more distinct zones of deposition. Shallower gradient fans are characterized as having a distinct depositional zone in the proximal sections, with more variability in the location and frequency of runout and depositional area as distance from the apex increases. This is interpreted as the variability in the threshold values of gradient. Debris flows will deposit at the gradient at which shear strength of the deposit exceeds the shear stresses related to the flow (Costa, 1984; Whipple and Dunne, 1992). Shallow gradient fans appear to be formed by more fluid debris flows with lower internal shear strengths. Steep fans appear to be formed by more viscous debris flows with generally higher internal shear strengths.

Acknowledgements

This material is based upon work supported by the National Science Foundation under Grant No. 0239749. Any opinions, findings, and conclusions or recommendations are those of the authors and do not necessarily reflect the views of the National Science Foundation. Special thanks go to the National Center for Airborne Laser Mapping (NCALM) for all of their assistance in data collection and post-processing. We would also like to thank Heather Volker for initial assistance with the original gridded DEM data. Two anonymous reviews provided comments that helped improve this manuscript.

References

Blackwelder, E., 1928. Mudflows as a geologic agent in semi-arid mountains. Geological Society of America Bulletin 39, 465–480.

Blaszczynski, J.S., 1997. Landform characterization with geographic information systems. Photogrammetric Engineering and Remote Sensing 63 (2), 183–191.

Costa, J.E., 1984. Physical geomorphology of debris flows. In: Costa, J.E., Fleisher, P.J. (Eds.), Developments and Applications of Geomorphology. Springer-Verlag, Berlin, pp. 268–317.

Fannin, R.J., Rollerson, T.P., 1993. Debris flows: some physical properties and behaviour. Canadian Geotechnical Journal 30, 71–81.

Lancaster, S.T., Hayes, S.K., Grant, G.E., 2003. Effects of wood on debris flow runout in small mountain watersheds. Water Resources Research 39 (6), ESG4-1–ESG4-21.

Larsen, M.C., Wieczorek, G.F., Eaton, L.S., Morgan, B.A., Torres-Sierra, H., 2001. Natural hazards on alluvial fans: the debris-flow and flash-flood disaster of northern Venezuela, December 1999. EOS, Transactions - American Geophysical Union 82 (47), 572–573.

Major, J.J., Iverson, R.M., 1999. Debris-flow deposition: effects of pore-fluid pressure and friction concentrated at flow margins. Geological Society of America Bulletin 111 (10), 1424–1434.

Okuda, S., Suwa, H., 1981. Topographical change caused by debris flow in Kamikamihori Valley, northern Japanese Alps. Transactions - Japanese Geomorphological Union 2, 343–352.

Parsons, J.D., Whipple, K.X., Simoni, A., 2001. Experimental study of the grain-flow, fluid–mud transition in debris flows. Journal of Geology 109, 427–447.

Suwa, H., Okuda, S., 1983. Deposition of debris flows on a fan surface of Mt. Yakedake, Japan. Zeitschrift fur Geomorphologie N.F. Supplementband 46, 79–101.

Whipple, K.X., Dunne, T., 1992. The influence of debris-flow rheology on fan morphology, Owens Valley, California. Geological Society of America Bulletin 104, 887–900.